

[Supplemental materials]

Calpain-6 confers atherogenicity to macrophages by dysregulating pre-mRNA splicing

Takuro Miyazaki,¹ Kazuo Tonami,² Shoji Hata,³ Toshihiro Aiuchi,⁴ Koji Ohnishi,⁵ Xiao-Feng Lei,¹ Joo-ri Kim-Kaneyama,¹ Motohiro Takeya,⁵ Hiroyuki Itabe,⁴ Hiroyuki Sorimachi,³ Hiroki Kurihara² and Akira Miyazaki¹

¹Department of Biochemistry, Showa University School of Medicine, 1-5-8 Hatanodai, Shinagawa-ku, Tokyo 142-8555, Japan

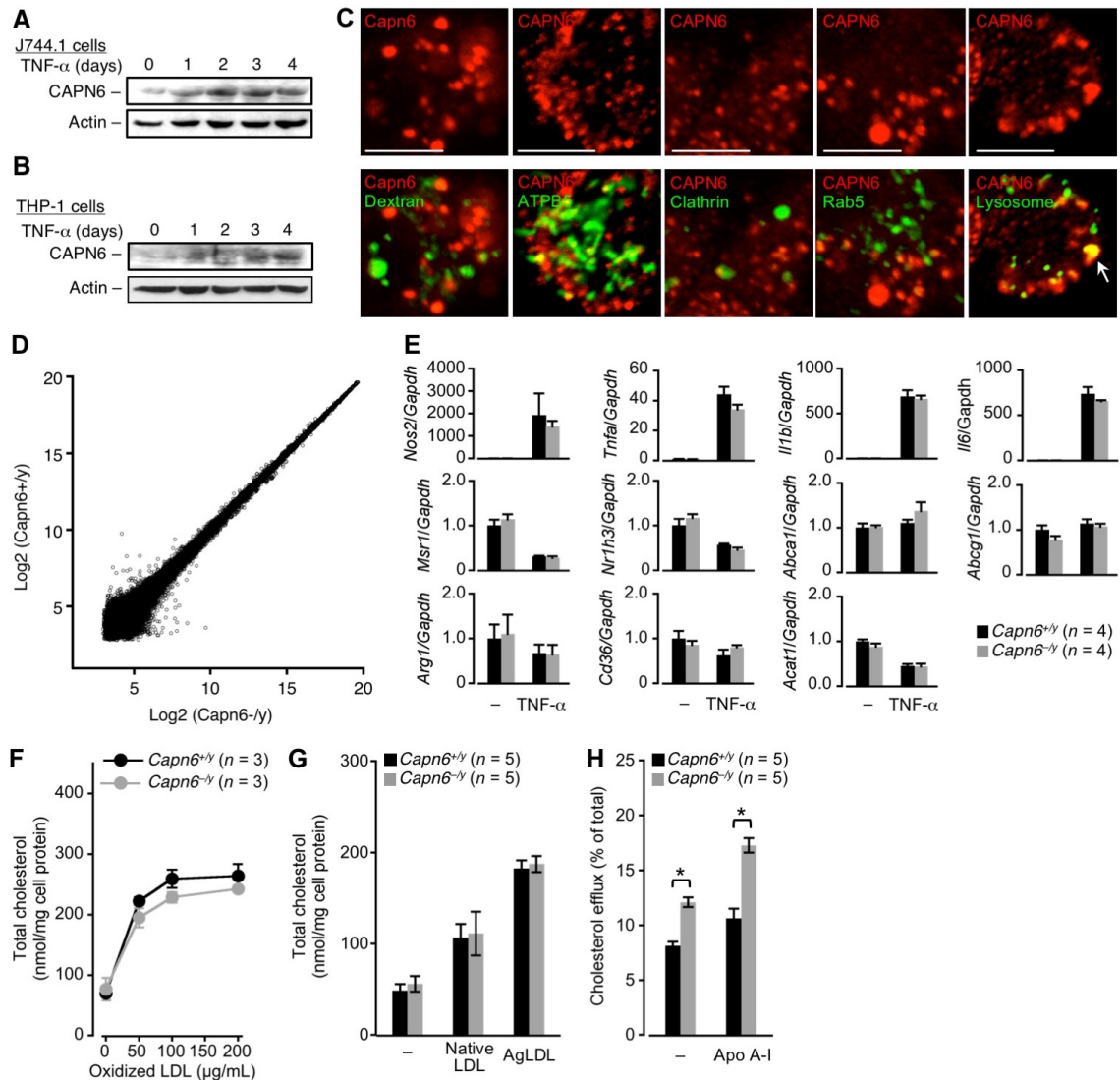
²Department of Physiological Chemistry and Metabolism, Graduate School of Medicine, The University of Tokyo, 7-3-1 Hongo, Bunkyo-ku, Tokyo 113-0033, Japan

³Calpain Project, Tokyo Metropolitan Institute of Medical Science, 2-1-6 Kamikitazawa, Setagaya-ku, Tokyo 156-8506, Japan

⁴Division of Biological Chemistry, Department of Molecular Biology, Showa University School of Pharmacy, 1-5-8 Hatanodai, Shinagawa-ku, Tokyo 142-8555, Japan

⁵Department of Cell Pathology, Graduate School of Medical Sciences, Faculty of Life Sciences, Kumamoto University, 1-1-1 Honjo, Chuo-ku, Kumamoto 860-8556, Japan

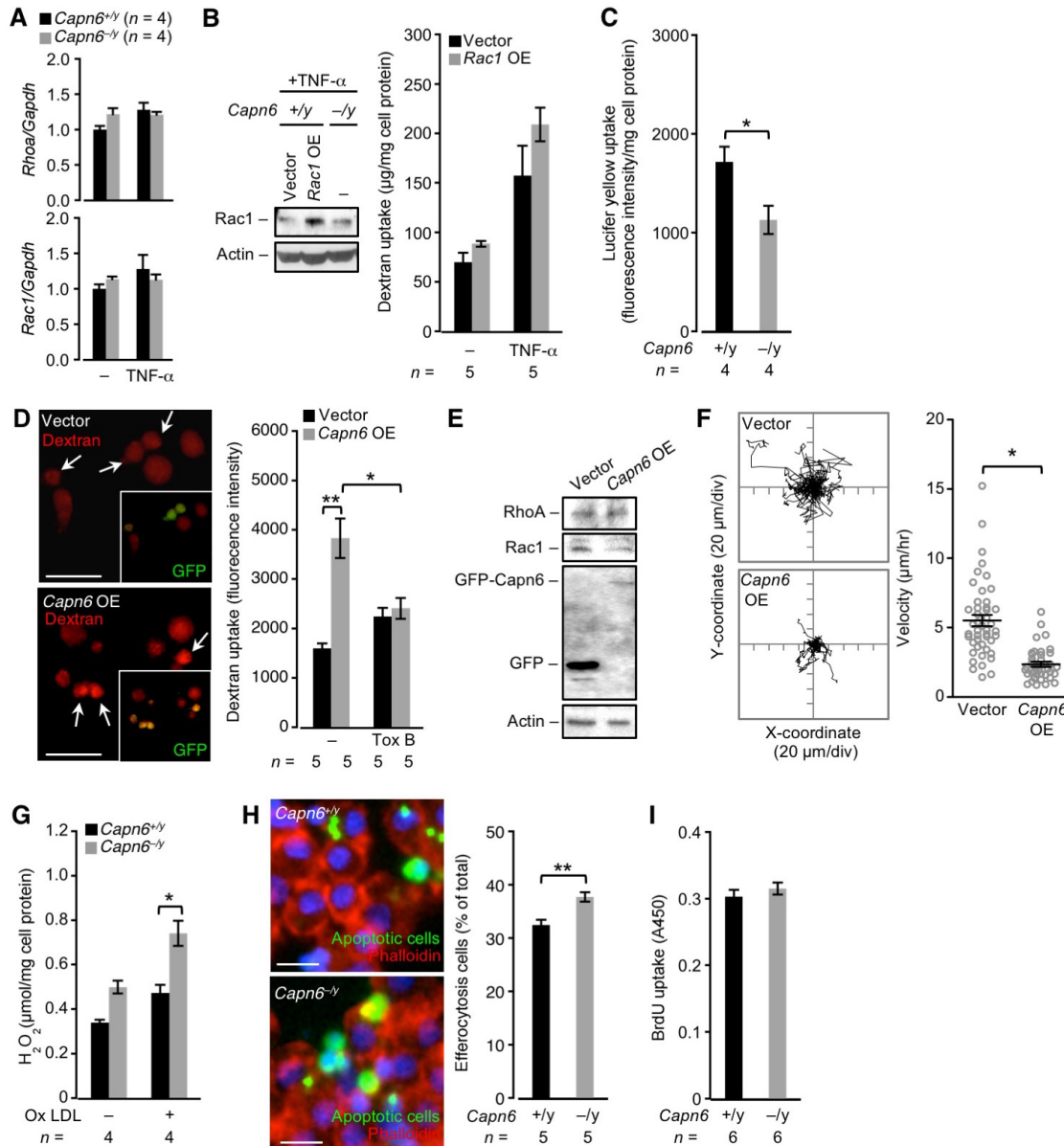
Supplemental Figures



Supplemental Figure 1. Related to Figure 1: Behavior and roles of calpain-6 in cultured macrophages.

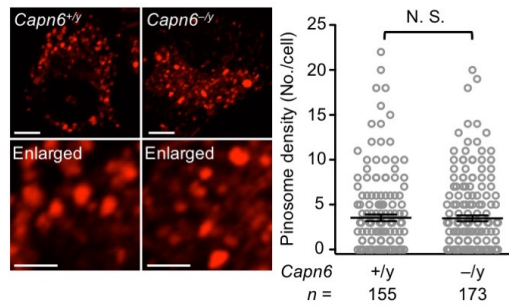
(A) Calpain-6 (CAPN6) in the murine macrophage cell line J774.1 was induced by macrophage colony stimulating factor (M-CSF)/tumor necrosis factor (TNF)- α stimulus. Cells were stimulated with M-CSF at 50 ng/mL and TNF- α at 10 ng/mL for the time periods indicated. (B) CAPN6 in the human monocytic THP-1 cell line was induced by M-CSF/TNF- α stimulus. Cells were stimulated with M-CSF at 50 ng/mL and TNF- α at 10 ng/mL for the time periods indicated. (C) CAPN6 in M-CSF/TNF- α -primed murine bone marrow-derived macrophages (BMMs) was not co-localized with pinosomes, mitochondria or endosomes. A small portion of CAPN6 overlapped with lysosomes. To label pinosomes, BMMs were incubated with tetramethylrhodamine-dextran for 30 min. ATP Synthase, H⁺ Transporting, Mitochondrial F1 Complex, Beta Polypeptide served as a marker of mitochondria. Clathrin and Rab5 served endosomal markers. Lysosomes were labeled by LysoTracker. Arrow indicates co-localization of CAPN6 with lysosome. (D) Scatter plot of DNA array data obtained by comparing the expression profiles between M-CSF/TNF- α -primed calpain-6 wild type (*Capn6*^{+/y}*Ldlr*^{-/-}) and deficient (*Capn6*^{-y}*Ldlr*^{-/-}) BMMs. Total RNA was harvested at Day 4 in the

differentiation processes. **(E)** Real-time reverse-transcription polymerase chain reaction analysis in M-CSF/TNF- α -primed *Capn6*^{+*y*}*Ldlr*^{-/-} and *Capn6*^{-*y*}*Ldlr*^{-/-} BMMs. Total RNA was harvested at Day 4 in the differentiation processes. **(F)** Uptake of oxidized LDL in TNF- α /M-CSF-primed *Capn6*^{+*y*}*Ldlr*^{-/-} or *Capn6*^{-*y*}*Ldlr*^{-/-} BMMs. Cells were treated with oxidized LDL for 24 h at the concentrations indicated. **(G)** Uptake of aggregated LDL in TNF- α /M-CSF-primed *Capn6*^{+*y*}*Ldlr*^{-/-} or *Capn6*^{-*y*}*Ldlr*^{-/-} BMMs. Cells were treated with native or aggregated LDL for 24 h at 100 μ g/mL. **(H)** ApoA-I-induced cholesterol efflux in TNF- α /M-CSF-primed *Capn6*^{+*y*}*Ldlr*^{-/-} or *Capn6*^{-*y*}*Ldlr*^{-/-} BMMs. NBD-cholesterol-loaded BMMs were incubated with 6 h in the presence or absence of apoA-I at 10 μ g/mL. * $p < 0.05$; one-way ANOVA followed by Bonferroni test **(H)**; Results are expressed as means \pm standard error; scale bars: 10 μ m **(C)**.



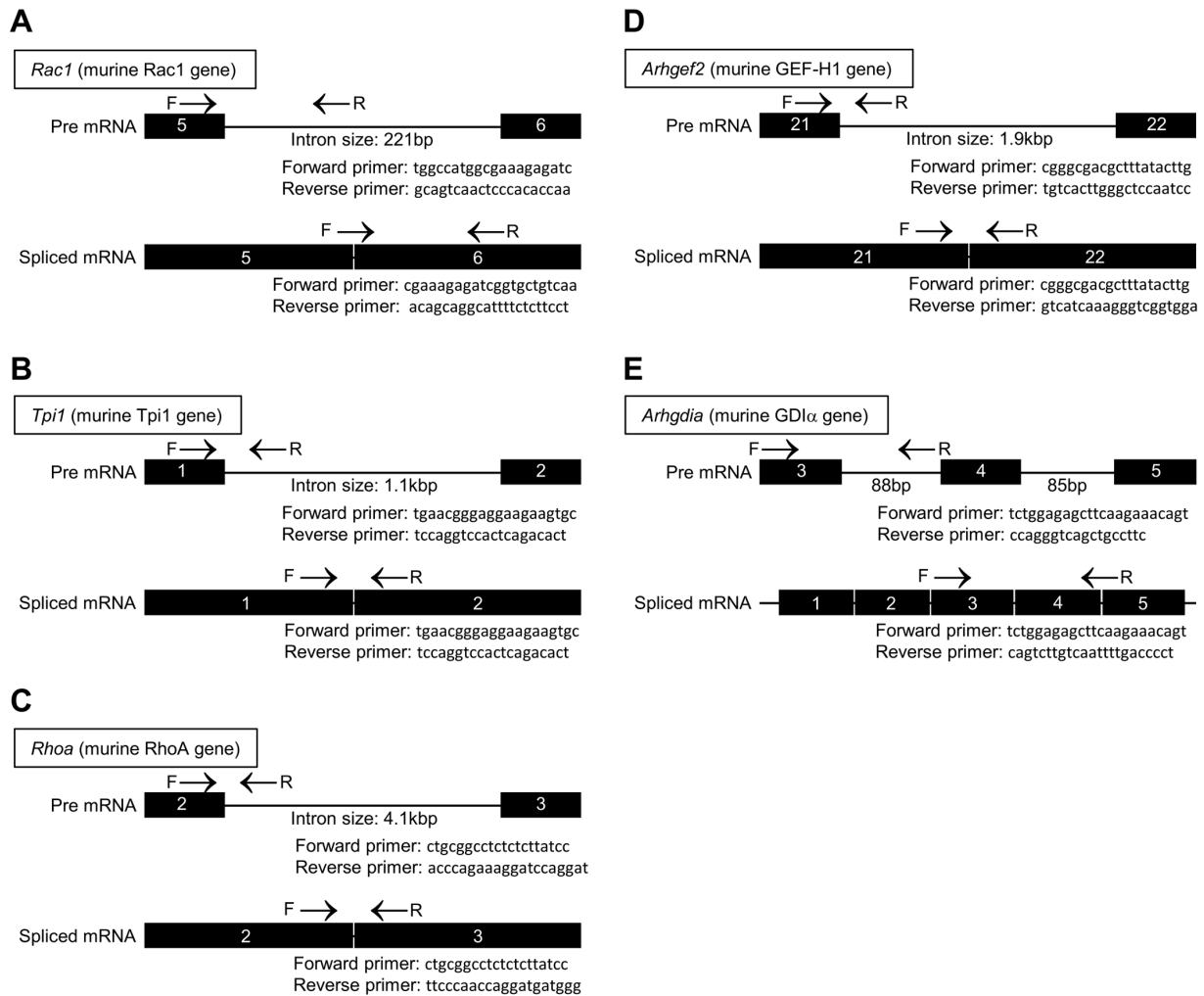
Supplemental Figure 2. Related to Figure 2: Roles of calpain-6 in pinocytotic activity, Rac1 expression, oxidative stress, efferocytosis and proliferation in cultured macrophages. (A) mRNA expression of *Ras* homolog gene family, member A and *RAS*-related C3 botulinus toxin substrate 1 in TNF- α /M-CSF-primed bone marrow-derived macrophages was unchanged by the deficiency of calpain-6 gene (*Capn6*). Total RNA was harvested at day 4 in the differentiation processes. Results are expressed as means \pm standard error. **(B)** Forced expression of Rac1 unchanged pinocytotic activity in *Capn6*^{+/-}*Ldlr*^{-/-} BMMs. **(C)** *Capn6* deficiency attenuated micropinocytosis in BMMs. Cells were subjected to Lucifer yellow at 0.5 mg/mL for 48 h. **(D)** Pinocytotic activity in *Capn6*-overexpressing J774 macrophages. Cells were pretreated with toxin B at 100 ng/mL for 24 h. Arrows represent GFP-expressing cells. **(E)** Rac1 protein expression in J774.1 cells declined following forced expression of *Capn6*. **(F)** Cellular movement in J774.1 cells was reduced by forced expression of *Capn6*. Cell movement was evaluated in the presence of chemokine (C-C motif) ligand 2 at 50 ng/mL. **(G)** Deficiency of *Capn6* accelerates production of H_2O_2 in BMMs. TNF- α /M-CSF-primed BMMs

were incubated for 2 h in the presence or absence of oxidized LDL at 100 $\mu\text{g}/\text{mL}$; then, the H_2O_2 was quantified by Amplex® Red-Hydrogen Peroxide/Peroxidase assay. **(H)** Loss of *Capn6* accelerates engulf of apoptotic cells in BMMs. X-ray irradiated apoptotic thymus cells were added to the BMM culture. Two hours later, the cells were washed three times and the effecrocytic BMMs were counted. **(I)** *Capn6* deficiency unaltered mitosis in BMMs. BrdU uptake in TNF- α /M-CSF-primed BMMs was measured as an index of proliferation. ** $p < 0.01$, * $p < 0.05$; Student's *t*-test (**C**, **F** and **H**) and one-way ANOVA followed by Bonferroni test (**D** and **G**); results are expressed as means \pm standard error; scale bars: 50 μm (**D**), and 20 μm (**H**).



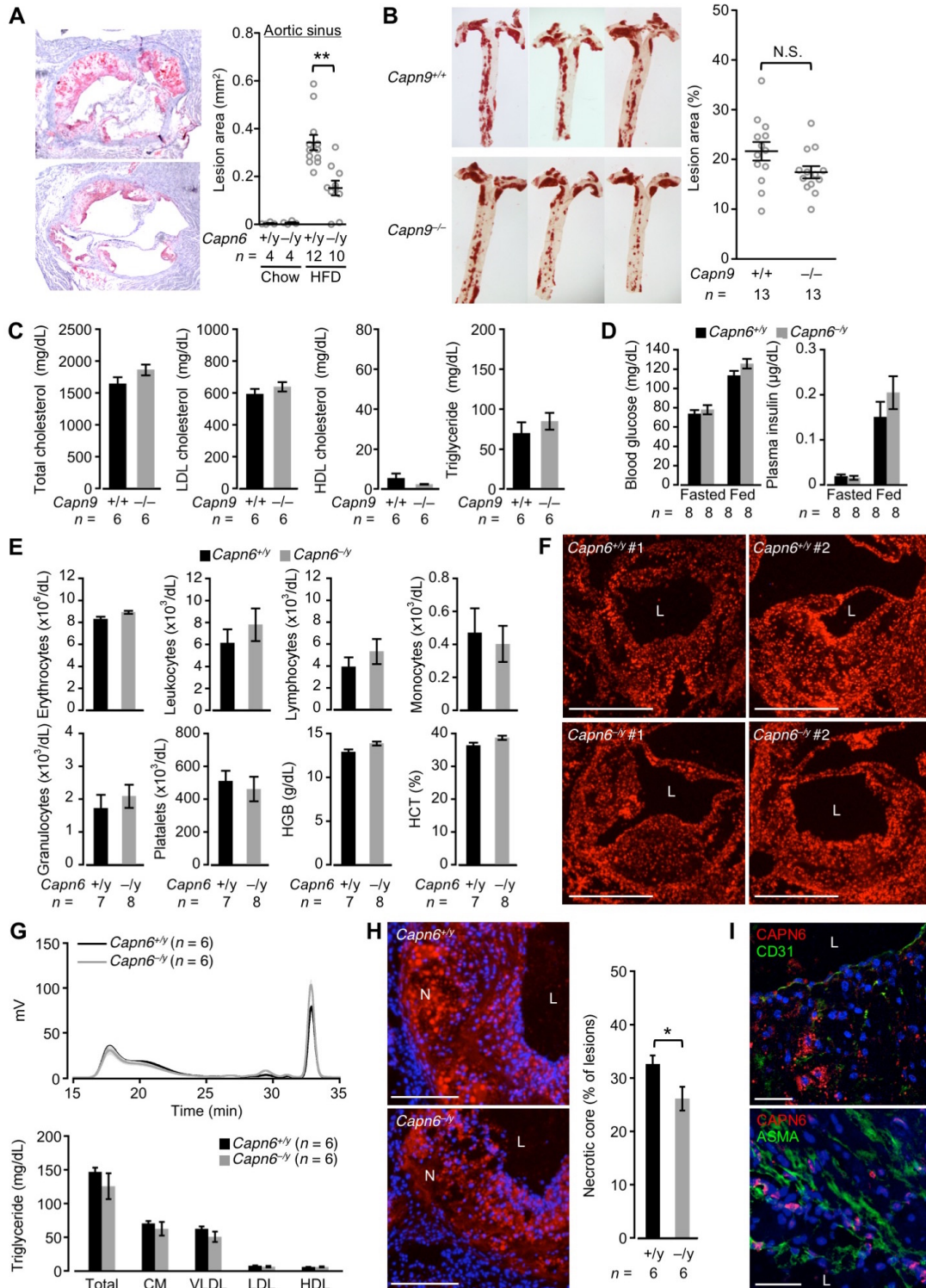
Supplemental Figure 3. Related to Figure 3: Deficiency of Calpain-6 unchanged pinosome density.

Pinosome density in Calpain-6 (*Capn6*)-deficient BMMs. The pinosome number per cell was counted. Error bars represent mean \pm SE; scale bars: 5 μ m (upper), and 3 μ m (lower).



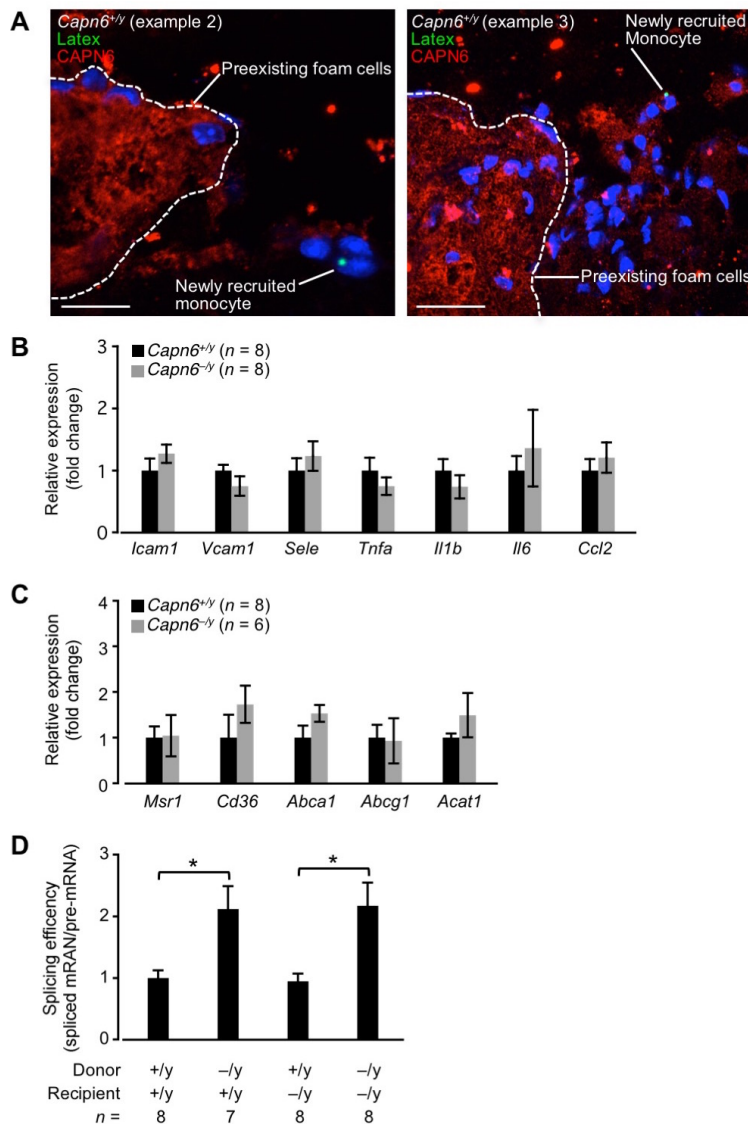
Supplemental Figure 4. Analytical principles of the polymerase chain reaction-based detection of mRNA splicing. Splicing efficiency was defined as the expression ratio of spliced mRNA to pre-mRNA. (A) To measure pre-*Rac1* mRNA, polymerase chain reaction (PCR) primers were designed to amplify the 3' end of fifth exon to the 5' end of the subsequent intron. To measure spliced *Rac1* mRNA, PCR primers were designed to amplify the boundary of the fifth/sixth exons and the 5' end of the sixth exon to avoid unexpected amplification of pre-*Rac1* mRNA by this primer pair. (B) To measure pre-*Tpi* mRNA, PCR primers were designed to amplify the 3' end of the first exon to the 5' end of the subsequent intron. To measure spliced *Tpi* mRNA, PCR primers were designed to amplify the 5' end of the first exon to the 3' end of the second exon because 1.1 kilobase pairs (kb) of the intron size is sufficient to distinguish spliced mRNA from pre-mRNA by dissociation analysis. (C) To measure pre-*Ras* homolog gene family, member A (*Rhoa*) mRNA, PCR primers were designed to amplify the 3' end of the second exon to the 5' end of the subsequent intron. To measure spliced *Rhoa* mRNA, PCR primers were designed to amplify the 5' end of the second exon to the 3' end of the third exon because 4.1 kb of the intron size is sufficient to distinguish spliced mRNA from pre-mRNA by dissociation analysis. (D) To measuring pre-*Arhgef2* mRNA, PCR primers were designed to amplify the 3' end of exon 21 to the 5' end of the subsequent intron. To measure spliced *Arhgef2* mRNA, PCR primers were designed to amplify the 5' end of exon 21 to the 3' end of exon 22 because 1.9 kb of the intron size is sufficient to distinguish spliced mRNA from pre-mRNA by dissociation analysis. (E) To

measure pre-*Arhgdia* mRNA, PCR primers were designed to amplify the internal region of the third exon and the subsequent intron. To measure spliced *Arhgef2* mRNA, PCR primers were designed to amplify the internal region of the third exon to the boundary of the fourth/fifth exons to avoid unexpected amplification of pre-*Arhgdia* mRNA by this primer pair.



Supplemental Figure 5. Related to Figure 7: Deficiency of calpain-6 or -9 in pro-atherogenic mice. (A) Calpain-6 (*Capn6*) deficiency reduces atherosclerotic plaques in aortic sinus in *Ldlr*^{-/-} mice. **(B)** Deficiency of calpain-9 gene (*Capn9*) did not affect atherogenesis in *Ldlr*^{-/-} mice. Aortic tissues were obtained from the mice that received HFD for 12 weeks. **(C)** Deficiency of calpain-9 gene (*Capn9*) did not affect plasma dyslipidemia in *Ldlr*^{-/-} mice. EDTA plasma was obtained from the mice that received HFD for 12 weeks. **(D)** Blood glucose and plasma insulin levels in *Capn6*^{+/-} and *Capn6*^{-/-} mice. The mice that received HFD for 12

weeks were fasted for 16 h, and were subsequently fed HFD for 2 h. **(E)** Blood cell population in *Capn6^{+y}Ldlr^{-/-}* and *Capn6^{-y}Ldlr^{-/-}* mice. EDTA-whole blood was analyzed by using VetScan hematology analyzer. **(F)** Oxidative stress in aortic atheromas in *Capn6^{+y}Ldlr^{-/-}* and *Capn6^{-y}Ldlr^{-/-}* mice. Dihydroethidium assay was performed in the mice received HFD for 12 weeks. L: aortic lumen. **(G)** Triglyceride levels in respective lipoprotein fractions in *Capn6^{+y}Ldlr^{-/-}* and *Capn6^{-y}Ldlr^{-/-}* mice. EDTA-plasma was collected in the mice received HFD for 12 weeks. **(H)** Necrotic core in aortic atheromas in *Capn6^{+y}Ldlr^{-/-}* and *Capn6^{-y}Ldlr^{-/-}* mice. Oil red-O staining was conducted to determine atheromas. DAPI-negative area in the atheromas served as a necrotic core. L: aortic lumen; N: necrotic core. **(I)** CAPN6 was not expressed in Cluster of differentiation 31 (CD31)-positive vascular endothelial cells and α -smooth muscle actin (ASMA)-positive cells in atherosclerotic lesions. Cryosections derived from *Ldlr^{-/-}* mice that received the HFD for 12 weeks were immunohistochemically analyzed. L: aortic lumen. **p < 0.01, *p < 0.05; one-way ANOVA followed by Bonferroni test **(A)** and Student's *t*-test **(H)**; results are expressed as means \pm standard error; scale bars: 400 μ m **(F)**, 200 μ m **(F)**, 100 μ m **(I, upper)** and 50 μ m **(I, lower)**.



Supplemental Figure 6 Related to Figure 10 and 11: Effects of calpain-6 deficiency on inflammatory responses and myeloid Rac1 splicing in atherosclerotic lesions. Total RNA for the qPCR analysis was derived from the aortas of mice that received a high-fat diet for 12 weeks. **(A)** Additional examples of CAPN6 expression in preexisting foam cell macrophages and newly-recruited monocytes. CAPN6 expression is abundant in the preexisting macrophages, but not in the newly-recruited monocytes, in *Capn6^{+/y}Ldlr^{-/-}* atheromas. **(B)** Deficiency of calpain-6 gene (*Capn6*) did not affect aortic inflammatory markers in *Ldlr^{-/-}* mice. **(C)** *Capn6* deficiency did not affect genes related to the receptor-mediated uptake of modified low-density lipoprotein in the aorta of *Ldlr^{-/-}* mice. **(D)** Myeloid CAPN6 was responsible for the elevation of *Rac1* mRNA splicing in atherosclerotic lesions. *Rac1* splicing efficiency in the whole aorta was compared between mice that received bone marrow transplantation. **p* < 0.05; one-way ANOVA followed by Bonferroni test **(D)**; Results are expressed as means ± standard error; scale bars: 20 μm (**A**, left), 40 μm (**A**, right).

Supplemental Table 1. Clinicopathological information for aortic autopsy specimens

Case No.	Age (years)	Sex	Diagnosis	Atherosclerotic grade
1	51	F	Endometrial sarcoma	Very mild
2	71	M	Hemophilia	Mild
3	67	F	Bone marrow embolism	Mild
4	86	F	Dilation of pulmonary artery	Mild-to-moderate
5	39	M	Staphylococcal infection	Moderate
6	68	F	Hepatocellular carcinoma	Moderate
7	65	M	Acute renal failure	Moderate
8	85	F	Thoracic aortic aneurysm	Moderate-to-severe
9	82	M	Acute occlusion of the superior mesenteric artery	Severe
10	69	M	Acute myocardial infarction	Severe

Supplemental Table 2. Clinicopathological information for tissue microarray

Case No.	Age (years)	Sex	Tissue	Atherosclerotic grade
1	69	M	Aorta	Normal
2	67	M	Coronary artery	Severe
3	73	F	RIVA nodule	Severe

Supplemental Table 3. Genotyping primers used in this study

Gene	Primer type	Sequences
<i>Capn6</i>	<i>Capn6</i> wild forward	5'-GCTCTCTACCACGATCCTTTATCC-3'
	<i>Capn6</i> wild reverse	5'-TTCTTCTTCCACAGCTGGCTGTAC-3'
	<i>Capn6</i> Neo forward	5'-CCACTCCCCTGTCCTTTCCTAAT-3'
	<i>Capn6</i> Neo reverse	5'-TTCTTCTTCCACAGCTGGCTGTAC-3'
<i>Capn9</i>	Sense	5'-CAGGGATCCCTGTGTCTGAAACCAGTC-3'
	Antisense	5'-GGAAGATACCCACATGGTGTGACACCA-3'
	Neo	5'-CTCGTGCTTTACGGTATCGCC-3'
<i>Ldlr</i>	Common	5'-CCATATGCATCCCCAGTCTT-3'
	<i>Ldlr</i> wild	5'-GCGATGGATACTCACTGC-3'
	Neo	5'-AATCCATCTTGTTCATGGCCGATC-3'

Supplemental Table 4. Antibodies used in this study

Immunogen	Product number/clone	Manufacturer	Dilution
For immunoblotting			
Calpain-6	KR084/-	Transgenic	1:100
Calpain-6	Ab38939/-	Abcam	1:1000
Rac1	ab155938/-	Abcam	1:1000
RhoA	sc-418/26C4	Santa Cruz Biotechnology	1:100
GEF-H1	ab90783/B4/7	Abcam	1:1000
RhoGDIa	ab133248/-	Abcam	1:1000
CWC22	bs-11464R/-	Bioss Antibodies	1:500
LaminB1	ab133741/-	Abcam	1:1000
β -Actin	ab6276/AC-15	Sigma	1:5000
For immunohistochemistry (mouse)			
Calpain-6	Ab38939/-	Abcam	1:100
Clathrin	610499/23	BD Transduction Laboratories	1:100
Rab5	610281/15	BD Transduction Laboratories	1:100
Rab11	610657/47	BD Transduction Laboratories	1:100
Cwc22 (rabbit antibody)	bs-11464R/-	Bioss Antibodies	1:100
Cwc22 (goat antibody)	sc-242525/K-20	Santa Cruz Biotechnology	1:100
Moma-2	MCA519G/MOMA-2	Bio-rad AbD Serotec	1:100
For immunohistochemistry (human)			
Calpain-6	Ab38939/-	Abcam	1:100
Cwc22	HPA036748/-	Sigma	1:100
CD68	H1405/PG-M1	Nichirei Bioscience	1:100

Supplemental Table 5. Polymerase chain reaction primers used in this study

Gene (gene symbol)	Forward primer	Reverse primer
Calpain-1 (<i>Capn1</i>)	5'-TGTCGTTCCGAGACTTCATCC-3'	5'-CGTCATCCACCTCCTCCAA-3'
Calpain-2 (<i>Capn2</i>)	5'-CACCTCACCTGTGACTCCTATAA-3'	5'-ATCCTCCTCATCTTCGTCTT-3'
Calpain-3 (<i>Capn3</i>)	5'-TGACGATGGCACGAACATGAC-3'	5'-AGTCTCTGAGCAGCGAGTTAT-3'
Calpain-5 (<i>Capn5</i>)	5'-CACCGACGACTCCCTTTACTA-3'	5'-GAGCTGATGCCATCTACGAAG-3'
Calpain-6 (<i>Capn6</i>)	5'-GGAAGCGTCCACAGGACATTT-3'	5'-TCATTGCCTTGTTCCTCAATC-3'
Calpain-7 (<i>Capn7</i>)	5'-GAAGGCCGCTACTCTGAGG-3'	5'-GGGCTTGCACTCTTTCCAGAT-3'
Calpain-8 (<i>Capn8</i>)	5'-AGAACTACCCAGCCACTTACTG-3'	5'-GCTCATCGGTGTGATTCTCCA-3'
Calpain-9 (<i>Capn9</i>)	5'-CCTTACCTGCATCGGTCCC-3'	5'-CTCAAACAAGGTGCCAGACTG-3'
Calpain-10 (<i>Capn10</i>)	5'-CGGGAGGACATCACTTGGAGA-3'	5'-AACTGCCAAATCCGACAGGTG-3'
Calpain-11 (<i>Capn11</i>)	5'-CTGCCATTGGCTCCCTTACC-3'	5'-GACCACGTTCAACCAGTGC-3'
Calpain-12 (<i>Capn12</i>)	5'-GAGGCTTCAACTCCGGTGG-3'	5'-GTTGCGCTGGATGAGTGACA-3'
Calpain-13 (<i>Capn13</i>)	5'-GACTTCAGGACCTTACGGGAT-3'	5'-CTTCTCGCCTATGGAAGATGC-3'
Calpain-15 (<i>Capn15</i>)	5'-ACAGTTGGGGAGTGGTCCT-3'	5'-GCTCCTCTACGCTGAGACGA-3'
Calpain-S1 (<i>CapnS1</i>)	5'-CGGAGTCATTAGCGCCATCAG-3'	5'-GTGTGCGGTACGACCTTG-3'
CD4 (<i>Cd4</i>)	5'-TCCTAGCTGTCACTCAAGGGA-3'	5'-TCAGAGAAGCTTCCAGGTGAAGA-3'
CD8a1 (<i>Cd8a1</i>)	5'-CTCTGGCTGGTCTTCAGTATGA-3'	5'-TCTTTGCCGTATGGTTGGTTT-3'
CD68 (<i>Cd68</i>)	5'-GACCTACATCAGAGCCCGAGT-3'	5'-CGCCATGAATGTCCACTG-3'
ICAM-1 (<i>Icam1</i>)	5'-GGCACCCAGCAGAAGTTGTT-3'	5'-CCTCAGTCACCTCTACCAAG-3'
VCAM-1 (<i>Vcam1</i>)	5'-TCTCTCAGGAAATGCCACCC-3'	5'-CACAGCCAATAGCAGCACAC-3'
E-selectin (<i>Sele</i>)	5'-TCCTCTGGAGAGTGGAGTGC-3'	5'-GGTGGGTCAAAGCTTCACAT-3'
IL-1 β (<i>Il1β</i>)	QuantiTect Primer Assay (QIAGEN) Mm_Il1b_2_SG (QT01048355)	
TNF- α (<i>Tnfα</i>)	QuantiTect Primer Assay (QIAGEN) Mm_Tnf_1_SG (QT00104006)	
IL-6 (<i>Il6</i>)	QuantiTect Primer Assay (QIAGEN) Mm_Il6_1_SG (QT00098875)	
CCL2 (<i>Ccl2</i>)	5'-CATCCACGTGTTGGCTCA-3'	5'-GATCATCTTGCTGGTGAATGAGT-3'
SR-A (<i>Msr1</i>)	5'-GCACAATCTGTGATGATCGCT-3'	5'-CCCAGCATCTTCTGAATGTGAA-3'
CD36 (<i>Cd36</i>)	5'-AGATGACGTGGCAAAGAACAG-3'	5'-CCTTGGCTAGATAACGAACTCTG-3'

ABCA1 (<i>Abcal</i>)	5'-GTTACGGCAGATCAAGCATCC-3'	5'-TGGAAGGGACAAATTGTGCTG-3'
ABCG1 (<i>Abcg1</i>)	5'-TCCTACTCTGTACCCGAGGG-3'	5'-CGGGGCATTCCATTGATAAGG-3'
ACAT1 (<i>Acat1</i>)	5'-CAGGAAGTAAGATGCCTGGAAC-3'	5'-TGCAGCAGTACCAAGTTTAGTG-3'
iNOS (<i>Nos2</i>)	5'-GTTCTCAGCCCAACAATACAAGA-3'	5'-GTGGACGGGTCGATGTCCAC-3'
LXR α (<i>Nr1h3</i>)	5'-CTCAATGCCTGATGTTTCTCCT-3'	5'-TCCAACCCTATCCCTAAAGCAA-3'
GAPDH (<i>Gapdh</i>)	5'-AGGTCGGTGTGAACGGATTTG-3'	5'-TGTAGACCATGTAGTTGAGGTCA-3'
HPRT1 (<i>Hprt1</i>)	5'-TGACACTGGCAAAAACAATGCA-3'	5'-GGTCCTTTTCACCAGCAAGCT-3'

Supplemental Table 6. Nucleotide sequences of short interfering RNAs

Gene	Details
Control RNA	Nonsilencing control RNA (medium GC; Invitrogen)
<i>Cwc22</i>	Stealth RNAi™ siRNA (Invitrogen) MSS246602
	Stealth RNAi™ siRNA (Invitrogen) MSS246603
	Stealth RNAi™ siRNA (Invitrogen) MSS246604
<i>Rac1</i>	Stealth RNAi™ siRNA (Invitrogen) MSS237707
	Stealth RNAi™ siRNA (Invitrogen) MSS237708

Supplemental Methods

Materials and reagents. Toxin B from *C. difficile* was purchased from List Biological Laboratories, Inc. (Campbell, CA, USA). Filipin III, γ -27632, and NSC23766 were obtained from Cayman Chemical Company (Ann Arbor, MI, USA). AngioSPARK was purchased from PerkinElmer. LysoTracker was obtained from Thermo Fisher Scientific. TRITC-dextran and nocodazol were purchased from Sigma-Aldrich Corp. TNF- α , IL-1 β , IL-4, CCL2, and IFN- γ were obtained from Peprotech, Inc. (Rocky Hill, NJ, USA). M-CSF (Leukoprol®) was purchased from Kyowa Hakko Kirin Co., Ltd. (Tokyo, Japan). Dil-labeled-LDL, oxidized LDL and apolipoprotein A-I (ApoA-I) derived from human plasma were obtained from Alfa Aesar (Ward Hill, MA, USA). Fluoresbrite® Plain YG Microspheres were purchased from Polysciences, Inc. (Warrington, PA, USA). Clodronate liposome was obtained from FormuMax Scientific Inc. (Sunnyvale, CA, USA). 25-[N-[(7-nitro-2-1,3-benzoxadiazol-4-yl)methyl]amino]-27-norcholesterol (25-NBD)-cholesterol was purchased from Avanti Polar Lipids Inc. (Birmingham, AL, USA). All other chemicals were commercial products of the highest available grade of purity. Human monocytic THP-1 cells were purchased from DS Pharma Biomedical (Osaka, Japan). J774 cells were a kind gift of Dr. Masamichi Takami (Showa University School of Dentistry, Tokyo, Japan).

Immunoblotting and nuclear fractionation. Immunoblotting was performed as described previously (1, 2, 3). Cells or aortic segments were lysed in ice-cold lysis buffer (125 mmol/L NaCl, 20 mmol/L Tris-HCl, 0.1% SDS, 1% Triton X-100, 1% sodium deoxycholate; pH 7.4) containing protease inhibitor cocktail (Sigma). A protein aliquot was subjected to electrophoresis on polyacrylamide gel containing SDS under reducing conditions; subsequently, proteins in the gel were transferred to a nitrocellulose membrane. The membranes were blocked with 5% nonfat dry milk (Cell Signaling Technology Japan, KK, Tokyo, Japan), after which they were reacted

overnight at 4°C with primary antibodies (Supplemental Table 4). After washing three times, membranes were incubated with horseradish peroxidase-conjugated anti-IgG mAbs. Next, proteins were detected with the ECL reagent (PerkinElmer). Extraction of the nuclear fraction was conducted using a Nuclear Extract Kit (Active Motif, Carlsbad, CA, USA) according to the manufacturer's instructions.

Immunoprecipitation. The cells transfected with vectors encoding GFP alone or GFP-fused *Capn6* using Lipofectamine® 3000 (Invitrogen, Carlsbad, CA, USA;). Cells were lysed on ice with lysis buffer (50 mmol/L Tris-HCl; pH7.5, 120 mmol/L NaCl, 0.5% Nonidet P-40, 40 µmol/L phenylmethylsulfonyl fluoride, 50 µg/mL leupeptin, 50 µg/mL aprotinin, 200 µmol/L sodiumorthovanadate, 1 mmol/L EGTA). For IgG capture, anti-GFP antibody (Clontech, Palo Alto, CA; 2 µg/reaction) were rotated with Dynabeads® Protein G (Invitrogen; 25 µL/reaction) in citrate phosphate buffer (24.5 mmol/L citric acid, 51.7 mmol/L dibasic sodium phosphate; pH 5.0) for 1 h at room temperature. Following washing three times with citrate phosphate buffer containing 0.1% Tween-20, the IgG-conjugated beads were magnetically separated and supplemented to the cell lysate, and were subsequently rotated for 1hr at room temperature. The beads were then washed three times by citrate phosphate buffer containing 0.1% Tween-20, and were eluted by boiling in sodium dodecyl sulfate (SDS) sample buffer (25 mmol/L Tris-HCl:pH 6.5, 5% glycerol, 1% SDS, 0.05% bromophenol blue, 3% 2-mercaptoethanol). Eluted proteins were analyzed by immunoblotting.

Uptake of aggregated LDL. BMMs at day 3 of differentiation in the presence of 10 ng/mL TNF- α and 50 ng/mL M-CSF were seeded on 48-well culture plate (2×10^5 cells/well). Aggregated LDL was prepared by vortexing native LDL for 2 min. Then, the cells were treated with native or aggregated LDL at 100 µg/mL for 24 h. After washing three times with Hank's balanced salt solution (HBSS), cellular lipids were extracted using hexane-isopropanol (v/v 3:2; 100 µL/well). Then, the extracts were transferred to another 96-well plate and dried. Cholesterol in the residue was quantified

using a Cholesterol-E Kit (Wako Pure Chemical Industries, Ltd.) and normalized against the total protein, which was measured by the bicinchoninic acid (BCA) method (Pierce Biotechnology, Inc., Rockford, IL, USA).

Cholesterol efflux. BMMs at day 3 of differentiation in the presence of 10 ng/mL TNF- α and 50 ng/mL M-CSF were seeded on 48-well culture plate (2×10^5 cells/well). The cells were incubated with RPMI medium supplemented with 25-NBD cholesterol (Avanti Polar Lipids Inc.) at 5 μ g/mL, ACAT inhibitor Sandoz 58-035 at 2 μ g/mL, TNF- α at 10 ng/mL and M-CSF at 50 ng/mL for 1 h. Then, the cells were washed three times, and were further incubated with RPMI medium supplemented with ACAT inhibitor Sandoz 58-035 at 2 μ g/mL, TNF- α at 10 ng/mL and M-CSF at 50 ng/mL in the presence or absence of ApoA-I at 10 μ g/mL. Subsequent to the incubation for 6 h, the culture medium was collected and cells were lysed by PBS containing 0.4% Triton X-100. Detached cells and unlysed debris in the culture medium and cell lysate were removed by centrifugation; then, fluorescence intensity in the culture medium or cell lysates was measured using a microplate reader (Mithras LB 940; Berthold Technologies GmbH & Co. KG, Bad Wildbad, Germany; Ex/Em: 490/515 nm). Cholesterol efflux was calculated from the following equation:

$$\text{Cholesterol efflux} = [F_{\text{media}} / (F_{\text{cell}} + F_{\text{media}})] \times 100\%,$$

where F_{media} represents fluorescence intensity in the culture medium, F_{cell} denotes fluorescence intensity in cell lysate.

Overexpression of Rac1. Expression vector containing full-length *Rac1* ORF (MC200361) was purchased from OriGene. BMMs at day 3 of differentiation in the presence of 10 ng/mL TNF- α and 50 ng/mL M-CSF were seeded on 12-well culture plate (1×10^6 cells/well). Then the cells were transfected with the expression vector or empty vector (2.5 μ g) using Lipofectamine® 3000 (Invitrogen) according to the manufacturer's instructions. Cells were subjected to experiments 24 h after transfection.

In vitro measurement of oxidative stress. BMMs at day 3 of differentiation in the

presence of 10 ng/mL TNF- α and 50 ng/mL M-CSF were seeded on 96-well culture plate (2×10^5 cells/well). Hydrogen peroxide that was released from the cells into the medium was quantified using an Amplex[®] Red-Hydrogen Peroxide/Peroxidase assay kit (Invitrogen) and normalized against the total protein, which was measured by BCA method (Pierce Biotechnology). Optical absorbance at 560 nm was measured as an index of hydrogen peroxide.

Efferocytosis. Efferocytotic activity in BMMs was determined according to the report by Tao *et al.* (4). BMMs at day 3 of differentiation in the presence of 10 ng/mL TNF- α and 50 ng/mL M-CSF were seeded on 48-well culture plate (2×10^5 cells/well). Then, isolated murine thymus cells were labeled by using Vybrant[®] CFDA SE Cell Tracer Kit (Invitrogen), and were irradiated with X-ray at 8 Gy using a soft X-ray system (OM-150HTS; OHMiC, Tokyo, Japan) to induce apoptosis; then, the apoptotic thymus cells (2×10^6 cells/well) were added to BMM culture. Following the incubation for 2 h, BMMs were washed three times with HBSS, and were fixed with 4% paraformaldehyde. The cells were counterstained with Texas Red[®]-labeled phalloidin (Invitrogen) and DAPI (Invitrogen), and were photographed by conventional fluorescence microscopy (IX70, Olympus, Japan). The number of efferocytotic cells was counted by using ImageJ software (National Institutes of Health [NIH], Bethesda, MD, USA), and was normalized by the total cell number in the observation fields.

BrdU uptake. BMMs at 4 day in differentiation in the presence of 10 ng/mL TNF- α and 50 ng/mL M-CSF were seeded on 96-well culture plate (1×10^5 cells/well). Proliferation of the cells in the presence of 10 ng/mL TNF- α and 50 ng/mL M-CSF was estimated by using BrdU Cell Proliferation ELISA kit (Abcam Inc., Cambridge, MA, USA) according to the manufacturer's instructions.

Blood glucose and plasma insulin. Glucose level in murine plasma was measured by using a glucose meter (Glutest pro GT-1660 equipped with Glutest Sensor; Sanwa Kagaku Kenkyusho, Nagoya). Plasma insulin concentration was determined by insulin

ELISA kit (Morinaga Institute of Biological Science, Inc., Yokohama, Japan).

Population of blood cells. EDTA-whole blood samples were isolated from the mice received HFD for 12 weeks. Blood cell population was analyzed by using VetScan hematology analyzer (ABAXIS, Sunnyvale, CA).

Oxidative stress in atherosclerotic lesions. Aortic sinus specimens were isolated from the mice that received HFD for 12 weeks. For measuring oxidative stress in atherosclerotic lesions, unfixed aortic cryosections (5 μm thickness) were incubated with dihydroethidium (Invitrogen) at 5 $\mu\text{mol/L}$ for 30 min at 37°C. Fluorescence intensity was measured as an index of proteolytic activity and oxidative stress. Images were acquired utilizing conventional fluorescent microscopy (IX70, Olympus, Japan) equipped with appropriate filter sets. Images were analyzed by using ImageJ software (NIH).

Measurement of plasma triglycerides. EDTA-plasma samples were isolated from the mice received HFD for 12 weeks. High-sensitivity lipoprotein profiling was performed on the plasma with the LipoSEARCH® system equipped with specific triglyceride detector by Skylight Biotech Inc. (Akita, Japan).

Necrotic core. Aortic sinus specimens were isolated from the mice that received HFD for 12 weeks, and were fixed with PBS supplemented 4% paraformaldehyde. Specimens were cryosectioned at the thickness of 5 μm , and were stained with Oil red-O at 3 mg/mL to visualize atherosclerotic lesions, together with the nuclear staining with DAPI. Fluorescence images were acquired utilizing conventional fluorescent microscopy (IX70, Olympus, Japan) equipped with appropriate filter sets. Images were analyzed by using ImageJ software (NIH). DAPI-negative area in the atheromas served as a necrotic core.

Real-time reverse-transcription polymerase chain reaction. Total RNA was isolated from aortic specimens or BMMs using TRIzol® Reagent (Invitrogen). cDNAs converted from the isolated RNA using ReverTra Ace® reverse transcriptase (Toyobo

Co., Ltd., Osaka, Japan) served as templates. Real-time reverse-transcription PCR was performed with GoTaq® DNA Polymerase (Promega Corp., Madison, WI, USA) using an ABI PRISM 7900 Sequence Detection System (Applied Biosystems, Waltham, MA, USA) with specific primers (Supplemental Table 5).

Transfection of short interfering RNAs. Following isolation, BMMs were cultured in the presence of M-CSF and TNF- α and were transfected with an siRNA (80 nmol/L) or a control RNA (80 nmol/L) using Lipofectamine® 3000 (Invitrogen) according to the manufacturer's instructions. The details of siRNAs are available in Supplemental Table 6. Cells were subjected to experiments 72 h after transfection.

DNA array. BMMs from four different mice were pooled in each mouse line to minimize the individual differences and were lysed using TRIzol® Reagent (Invitrogen). Total RNA was extracted from the lysates, and the quality of this total RNA was validated using a 2100 BioAnalyzer (Agilent Technologies, Santa Clara, CA, USA). The DNA array was conducted using an Agilent Expression Array (Agilent Technologies) and a SurePrint G3 Mouse GE 8 \times 60 K Microarray (Agilent Technologies) in the Dragon Genomics Center (Takara Bio Inc.). Data are available in the NCBI's Gene Expression Omnibus (GEO) database (GEO GSE83815).

Supplemental References

1. Kigawa Y, Miyazaki T, Lei XF, Nakamachi T, Oguchi T, Kim-Kaneyama JR, Taniyama M, Tsunawaki S, Shioda S, Miyazaki A. NADPH oxidase deficiency exacerbates angiotensin II-induced abdominal aortic aneurysms in mice. *Arterioscler Thromb Vasc Biol.* 2014;34(11):2413–2420.
2. Miyazaki T, Taketomi Y, Takimoto M, Lei XF, Arita S, Kim-Kaneyama JR, Arata S, Ohata H, Ota H, Murakami M, Miyazaki A. m-Calpain induction in vascular endothelial cells on human and mouse atheromas and its roles in VE-cadherin disorganization and atherosclerosis. *Circulation.* 2011;124(23):2522–2532.
3. Miyazaki T, Taketomi Y, Saito Y, Hosono T, Lei XF, Kim-Kaneyama JR, Arata S, Takahashi H, Murakami M, Miyazaki A. Calpastatin counteracts pathological angiogenesis by inhibiting suppressor of cytokine signaling 3 degradation in vascular endothelial cells. *Circ Res.* 2015;116(7):1170–1181.
4. Tao H, Yancey PG, Babaev VR, Blakemore JL, Zhang Y, Ding L, Fazio S, Linton MF. Macrophage SR-BI mediates efferocytosis via Src/PI3K/Rac1 signaling and reduces atherosclerotic lesion necrosis. *J Lipid Res.* 2015;56(8):1449-60.